

## Fragment spin as a function of the mass asymmetry in heavy ion induced fission reactions

R. K. Choudhury, A. Saxena, A. Chatterjee, D. V. Shetty, and S. S. Kapoor  
*Nuclear Physics Division, Bhabha Atomic Research Centre, Mumbai 400085, India*

M. Cinausero, L. Corradi, E. Farnea, E. Fioretto, A. Gadea, D. Napoli, G. Prete, and A. M. Stefanini  
*Laboratori Nazionali di Legnaro, Legnaro, Italy*

D. Bazzaco, S. Beghini, D. Fabris, G. Montagnoli, G. Nebbia, C. Rossi-Alvarez, F. Scarlassara, C. Ur, and G. Viesti  
*Dipartimento di Fisica dell'Università and INFN, Sezione di Padova, Padova, Italy*  
 (Received 30 March 1999; published 4 October 1999)

The total average spins of fission fragments were measured as a function of fragment mass in  $^{12}\text{C}$ ,  $^{16}\text{O} + ^{209}\text{Bi}$  and  $^{12}\text{C}$ ,  $^{16}\text{O} + ^{232}\text{Th}$  reactions at bombarding energies near and above the Coulomb barrier. The mass dependence of the fragment spin for the  $^{12}\text{C}$ ,  $^{16}\text{O} + ^{232}\text{Th}$  reactions is observed to be in marked contrast to that for the  $^{12}\text{C}$ ,  $^{16}\text{O} + ^{209}\text{Bi}$  reactions. The present results have been analyzed within the framework of the statistical model taking into account the finite relaxation times for the equilibration of the collective-spin modes. The observed features in  $^{12}\text{C}$ ,  $^{16}\text{O} + ^{232}\text{Th}$  reactions can be ascribed to incomplete equilibration of the collective-spin modes where the mass relaxation at extreme mass asymmetries terminates before full statistical equilibration of the collective-spin modes is reached. [S0556-2813(99)04110-2]

PACS number(s): 25.70.Jj, 24.60.-k

### I. INTRODUCTION

Studies of spin distributions of fission fragments provide important information on the mechanism of spin inducement and the excitation of collective degrees of freedom in the fission process. In heavy-ion-induced fission reactions, the fragments acquire a certain amount of angular momentum due to the fractionation of the initial compound nucleus spin into the aligned components known as the rigid rotation and the tilting ( $K$ ) components. In addition, the fission fragments also acquire spin by the statistical excitation of various angular momentum bearing modes, such as wriggling, bending, and twisting of the fissioning nucleus at the scission point [1]. These modes are excited even when the fissioning system does not possess any net angular momentum as in central collisions or in the  $^{252}\text{Cf}$  spontaneous fission. The angular momentum bearing collective modes influence the final fragment spins in two ways: (i) they enhance the fragment spin over that of rigid rotation predicted by the simple concepts of rolling and sticking, and (ii) they introduce a randomly oriented component of angular momentum which produces a misalignment of the fragment spin in a plane perpendicular to the fission axis. These effects have been studied in the past [2–5] in a number of fusion-fission reactions by measuring the fission fragment spin from the  $\gamma$ -ray multiplicity measurements. These studies have indicated that the angular momentum bearing collective modes are fully equilibrated in the fission process. Schmitt *et al.* [2] have investigated  $^{12}\text{C}$ ,  $^{20}\text{Ne}$ , and  $^{40}\text{Ar}$  induced fission reactions and found the  $\gamma$ -ray multiplicity to be essentially independent of the mass split. This feature could be explained within the framework of the statistical model, which assumes that all the angular momentum bearing collective modes are excited in the fragments in a statistically independent manner. The weak dependence of  $\gamma$ -ray multiplicities on mass asymmetry was understood to be the result of two opposing fac-

tors: the increase of the spin component due to the rigid rotation and the decrease in the spin component by collective modes with increasing mass asymmetry. A similar weak dependence was found for several  $^{208}\text{Pb}$ -induced reactions by Bock *et al.* [3].

Recently, there have been observations of several anomalous features in the fission characteristics in heavy-ion-induced fission reactions, such as anomalously large fission fragment angular anisotropies and anomalously large widths in mass distribution, etc., which have been interpreted as due to the occurrence of nonequilibrium fission modes in the fission process. Studies on the fragment angular distributions in many systems involving actinide target nuclei such as  $^{232}\text{Th}$  and  $^{238}\text{U}$  show anomalous fission anisotropies at near and sub-barrier energies [6–15]. The large fission anisotropies are understood to be caused by the presence of a certain fraction of quasifission or pre-equilibrium fission due to the interaction of the projectile along the elongated axis of the deformed target nucleus. The presence of a nonequilibrium fission component, characterized by a narrow  $K$  distribution at the saddle point along with the normal fission events, gives rise to higher angular anisotropies. Similarly the dependence of  $\gamma$ -ray multiplicity on fragment mass asymmetry, seen in some recent works, is difficult to reconcile with the statistical equilibration of the collective modes alone. In some cases, a maximum is observed at symmetry, while in others they are essentially independent of mass split [3–5]. Masri *et al.* [16] have studied the reactions of 220 MeV  $^{20}\text{Ne} + ^{\text{Nat}}\text{Re}$  and 315 MeV  $^{40}\text{Ar} + ^{165}\text{Ho}$ . The two reactions lead to the same fused nucleus  $^{205}\text{At}$  at the same excitation energy (167 MeV). The critical angular momentum for capture (i.e., fusion-fission plus quasifission) in the Ne + Re system is  $(91 \pm 3) \hbar$  which is close to  $l_{Bf}=0$  ( $\sim 80\hbar$ ) (the angular momentum at which the fission barrier goes to zero), whereas for the Ar + Ho reaction the critical angular momentum for capture is  $(136 \pm 4) \hbar$  which is much larger than

the  $l_{Bf}=0$ , favoring the occurrence of a fast fission process. It was observed that the average  $\gamma$ -ray multiplicity as a function of fragment mass has a more pronounced minimum at the symmetry for the Ar+Ho system as compared to the Ne+Re system. This effect was interpreted on the basis of the nonequilibration of the tilting mode due to the fast fission process.

Back *et al.* [17] have studied a large number of systems such as  $^{238}\text{U}+^{16}\text{O}$ ,  $^{26}\text{Mg}$ ,  $^{27}\text{Al}$ ,  $^{32}\text{S}$ ,  $^{35}\text{Cl}$ ,  $^{40}\text{Ca}$ ,  $^{48}\text{Ca}$ , and  $^{nat}\text{Zn}$  at energies of 5.4, 5.9, 6.7, and 7.5 MeV/nucleon. The heavier systems exhibited a pronounced n shape in the mass dependence of the fragment spin, with the exception of the  $^{238}\text{U}+^{16}\text{O}$  reaction, which was explained to be due to presence of quasifission events in these reactions. In quasifission reactions, full statistical equilibrium of fragment spin is not reached for the asymmetric mass divisions.

In order to investigate the nonequilibrium aspects in the fission process, it is of interest to study the fragment spin as a function of fragment mass for the systems which exhibit anomalous angular anisotropies at near and sub-barrier energies. Consequently, we have carried out in the present work the measurements of fission fragment spins in  $^{12}\text{C}$ ,  $^{16}\text{O}+^{232}\text{Th}$  reactions as a function of fragment mass over a broad range of bombarding energies. The  $^{12}\text{C}$ ,  $^{16}\text{O}+^{209}\text{Bi}$  systems were also studied for comparison with the  $^{232}\text{Th}$  systems. The results were analyzed on the basis of the statistical model to decipher the contributions of various excitation modes to the fragment spin as a function of fragment mass. The paper is organized as follows. The following section gives the experimental details and the results obtained from the present measurements. Section III contains the statistical model analysis for the calculation of the fragment spin as a function of mass split. The discussions of the present results are given in Sec. IV. Section V gives the summary and conclusions of the present study.

## II. EXPERIMENTAL DETAILS AND RESULTS

The measurements were carried out at the XTU Tandem accelerator facility of the Laboratori Nazionali di Legnaro. Beams of  $^{12}\text{C}$  and  $^{16}\text{O}$  were used to bombard self-supporting targets of  $1.5\text{ mg/cm}^2$   $^{232}\text{Th}$  and  $500\text{ }\mu\text{g/cm}^2$   $^{209}\text{Bi}$ . The  $\gamma$  rays were detected with the  $\gamma$ -ray spectrometer array GASP [18], which consists of 40 large volume Compton suppressed Ge detectors and an inner ball of 80 bismuth germanate (BGO) crystals. In this work the BGO detectors were used for the determination of the  $\gamma$ -ray multiplicities in the fission process. The average absolute efficiency of individual BGO detectors was determined using  $^{60}\text{Co}$  and  $^{152}\text{Eu}$  sources to be  $\epsilon=0.0098$ . Two multiwire proportional counters (MWPC) having active area of  $10\times 8\text{ cm}^2$  were placed in plane at a distance of 8 cm from the target at  $\theta_{\text{lab}}=\pm 90^\circ$  with respect to the beam direction. The MWPC's were used to detect the two coincident fission fragments. These detectors were operated at a gas pressure of 5 mbar and provided good pulse height discrimination of fission fragments from elastically scattered particles.

Coincidence between the two MWPC detectors and the GASP detectors was required to collect the data. The timing

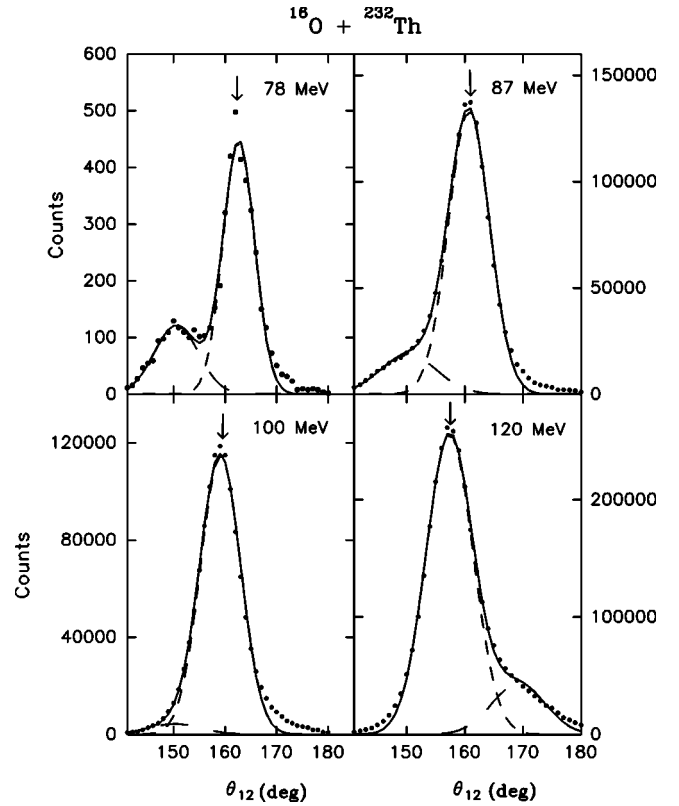


FIG. 1. Typical folding angle distributions for the  $^{16}\text{O}+^{232}\text{Th}$  reaction. The arrows in the figure indicate the expected value of the folding angle for full linear momentum transfer. The solid curve shows the sum of the contributions of full momentum transfer (short-dashed curve) and incomplete momentum transfer (long-dashed curve) events.

and energy signals of the individual  $\gamma$ -ray detectors and the position and the time difference signals from the two MWPC detectors were recorded for each event. Only the data relative to coincidences with the BGO detectors are presented in this work.

The position signals from the MWPC detectors were transformed event by event to polar and azimuthal angles  $(\theta, \phi)$ . The  $\theta$  values were added to give the fragment folding angle. Figure 1 shows typical folding angle distributions for the  $^{16}\text{O}+^{232}\text{Th}$  reaction at selected bombarding energies. It can be seen that the measured folding angle distributions are dominated by full linear momentum transfer (FLMT) events except for a small component of transfer-induced fission events seen as a hump on both sides of the FLMT peak. At higher energies, this incomplete fusion component appears at larger folding angles whereas at sub-barrier energies they correspond to smaller folding angles as compared to the FLMT events. The data on the  $\gamma$ -ray multiplicity and mass distributions of fission fragments presented in the following were obtained by selecting the FLMT events in the folding angle distributions.

The fragment masses were determined from the time difference between the MWPC detector signals using the following expressions:

$$m_1 = [(t_1 - t_2) + m_{\text{CN}}d_2] / (d_1/p_1 + d_2/p_2), \quad (1)$$

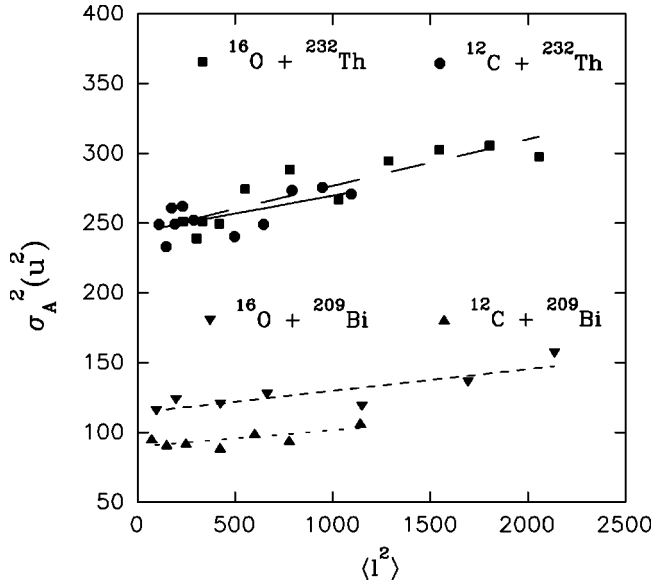


FIG. 2. Variance of the mass distribution as a function of mean-square angular momentum for  $^{12}\text{C}$ ,  $^{16}\text{O} + ^{232}\text{Th}$  and  $^{12}\text{C}$ ,  $^{16}\text{O} + ^{209}\text{Bi}$  reactions. The dashed lines in the figure are the least-squares fit to the data.

$$m_2 = m_{\text{CN}} - m_1, \quad (2)$$

$$p_1 = m_{\text{CN}} v_{\text{CN}} / [\cos \theta_1 + \sin \theta_1 \cot \theta_1], \quad (3)$$

and

$$p_2 = p_1 \sin \theta_1 / \sin \theta_2, \quad (4)$$

where  $m_1$ ,  $m_2$  are the fragment masses,  $t_1$ ,  $t_2$  are flight times of the fragments for the distances  $d_1$  and  $d_2$  respectively, at which the two complementary fragments are detected in the MWPC detectors,  $p_1$  and  $p_2$  are the linear momenta in the laboratory of the two fragments. The mass and velocity of the compound nucleus are indicated as  $m_{\text{CN}}$  and  $v_{\text{CN}}$ , respectively. The masses determined directly from the velocity of the fragments are not affected, on the average, by sequential neutron emission from the fission fragments. It is found that the reconstructed mass distributions are of Gaussian shape peaked around the symmetric mass for all the systems. The variances of the fragment mass distribution  $\sigma_A^2$ , are shown in Fig. 2 for the  $^{12}\text{C}$ ,  $^{16}\text{O} + ^{232}\text{Th}$  and  $^{12}\text{C}$ ,  $^{16}\text{O} + ^{209}\text{Bi}$  systems as a function of the entrance channel angular momentum  $\langle l^2 \rangle$  corresponding to each bombarding energy. The  $\langle l^2 \rangle$  values were determined from CCFUS calculations [19]. The  $\sigma_A^2$  values are found to increase linearly with  $\langle l^2 \rangle$  as observed in earlier studies [20]. The dashed lines in the figure are the least-squares fit to the data for various systems. It is also observed in Fig. 2 that the mass distributions are considerably wider for the more fissile systems populated with  $^{232}\text{Th}$  target as compared to the ones corresponding to the  $^{209}\text{Bi}$  target.

Figure 3 shows typical  $\gamma$ -ray fold distributions for the  $^{16}\text{O} + ^{232}\text{Th}$  reactions at selected bombarding energies. As expected, there is a systematic lowering of the peak value of the fold distribution with decreasing bombarding energy. In

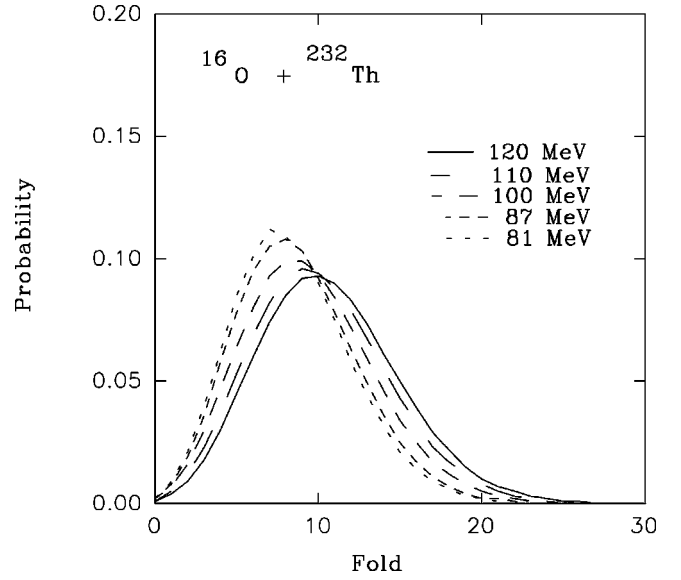


FIG. 3. Typical fold distributions for the  $^{16}\text{O} + ^{232}\text{Th}$  reaction at selected bombarding energies.

order to derive the average  $\gamma$ -ray multiplicities from the measured fold distributions, we have used the method suggested by Ockels [21]. The derived average  $\gamma$ -ray multiplicity without selection of the fragment mass, shows a steady increase with bombarding energy for all the reactions studied. The present results are in good agreement with the earlier measurements reported in the literature [22–24]. Figure 4 shows average  $\gamma$ -ray multiplicities  $\langle M \gamma \rangle$  as a function of bombarding energy for selected mass windows for various systems. It is observed that while the  $\langle M \gamma \rangle$  values for symmetric splitting (shown by open circles) are higher compared to the asymmetric ones for all the reactions studied, the difference between symmetric and asymmetric splittings depends significantly on the bombarding energy. Furthermore, the mass dependence of  $\langle M \gamma \rangle$  is observed to be strikingly different for the reactions on the  $^{232}\text{Th}$  target as compared to those on  $^{209}\text{Bi}$ . In the case of  $^{232}\text{Th}$  target, the mass dependence of the average  $\gamma$ -ray multiplicity is quite weak at low bombarding energies, and becomes stronger with increase in the bombarding energy. Whereas, in case of  $^{12}\text{C}$ ,  $^{16}\text{O} + ^{209}\text{Bi}$  reactions, an opposite trend is evidenced, i.e., there is an appreciable dependence of  $\langle M \gamma \rangle$  on the fragment mass at low energies and almost no dependence at the highest energies. This contrasting feature is more clearly brought out in Figs. 5 and 6, where we have plotted the average fragment spin as a function of fragment mass for different bombarding energies for the  $^{209}\text{Bi}$  and  $^{232}\text{Th}$  systems, respectively. It may be mentioned that the conversion from  $\gamma$ -ray multiplicity to total fragment spin may involve some uncertainties. The conversion suffers from the lack of knowledge on the average multipolarities ( $E1$ ,  $M1$ ,  $E2$ ) of the  $\gamma$ -ray transitions and the spin removed by the evaporated particles during the fission process. In view of these difficulties, we have adopted the simple conversion relation  $\langle S_T \rangle \approx 2.0 \langle M \gamma \rangle$ , as assumed in the earlier works [2,17]. In Figs. 5 and 6, the

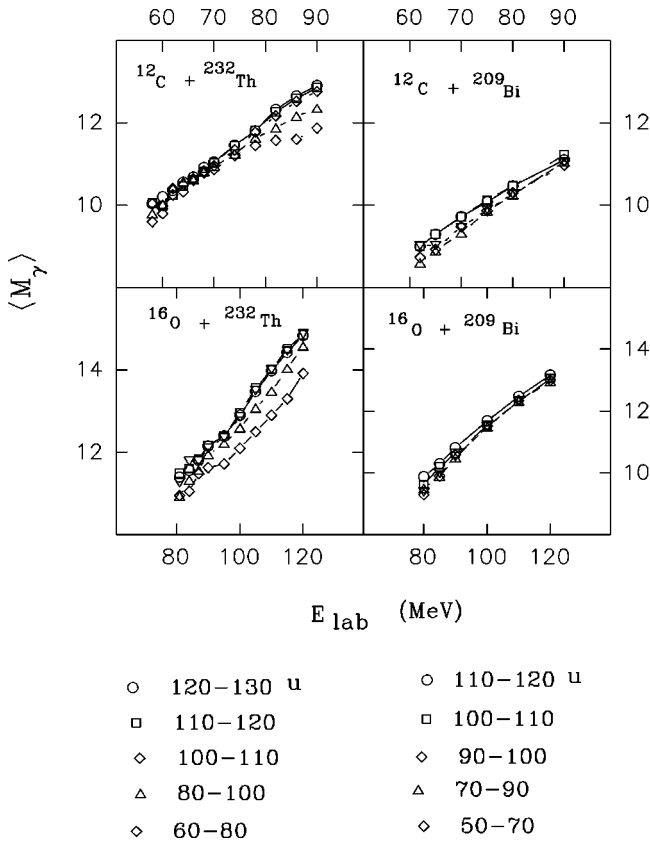


FIG. 4. Average  $\gamma$ -ray multiplicity as a function of bombarding energy for different mass windows.

measured data have been reflected around the symmetric splitting to show the mass dependence for both light and heavy fragments.

The data shown in Figs. 5 and 6 clearly indicate that the average total fragment spin is fairly independent of the fragment mass for the  $^{12}\text{C}$ ,  $^{16}\text{O}+^{209}\text{Bi}$  reactions at all the measured energies. On the other hand, there is an n-shaped dependence of the fragment spin on fragment mass for the  $^{12}\text{C}$ ,  $^{16}\text{O}+^{232}\text{Th}$  reactions at higher bombarding energies. As noted above, a similar observation was reported by Back *et al.* [17] in a number of  $^{238}\text{U}$ -induced fission reactions.

### III. STATISTICAL MODEL ANALYSIS

The theoretical treatment for the determination of fragment spin due to wriggling, bending, tilting, and twisting modes as a function of fragment mass asymmetry has been discussed by Schmitt and Pacheco [1,25] in the framework of the statistical model. The collective-spin modes in the statistical model are assumed to be in statistical equilibrium and are independently excited. The rigid rotation contribution to the total fragment spin is coupled to these angular momentum bearing collective modes. The relevant expressions used for calculating the average fragment spins due to various collective modes can be found in Refs. [1,25]. The determination of fragment spin using these expressions requires the following inputs:

- (1) The initial  $l$  distribution of the compound nucleus.

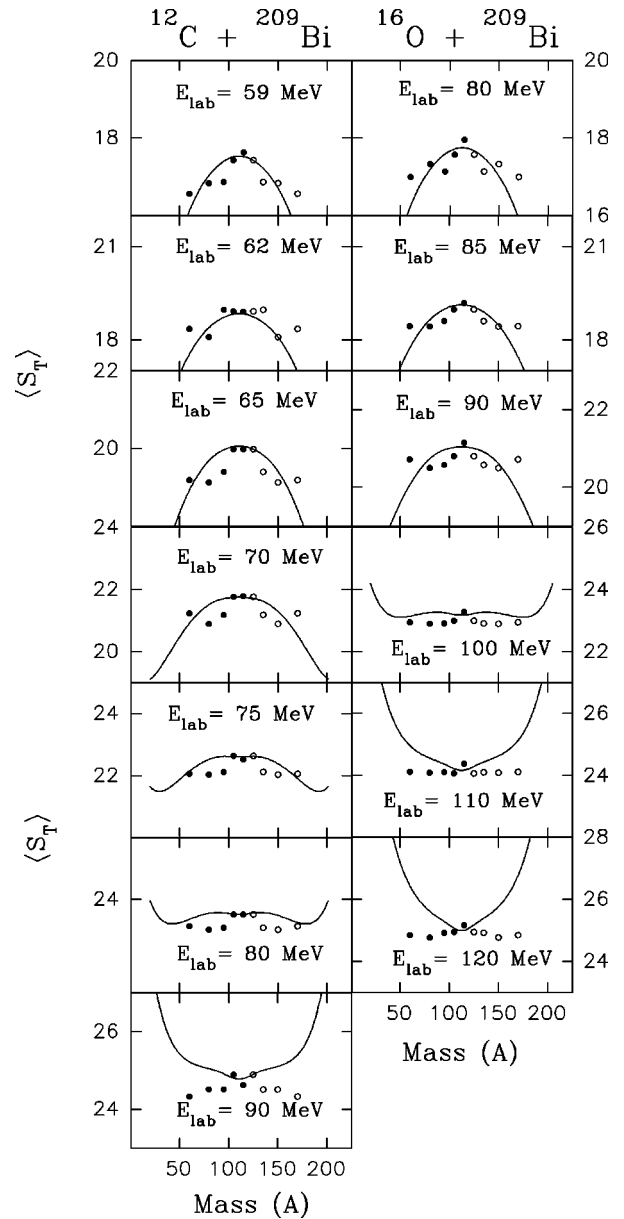


FIG. 5. Average total spin as a function of fragment mass at various bombarding energies for  $^{12}\text{C}+^{209}\text{Bi}$  and  $^{16}\text{O}+^{209}\text{Bi}$  reactions. The solid curves in the figure correspond to the statistical model calculations of Schmitt *et al.* [25].

- (2) The moments of inertia of the fission fragments.
- (3) The excitation energy or the temperature of the fissioning nucleus.

The initial  $l$  distributions of the compound nucleus were obtained from the CCFUS calculations, which account well for the experimentally measured fusion excitation functions for all the present systems. The determination of excitation energy of the fissioning nucleus may have some uncertainty due to the assumption of whether the calculations are to be done at the saddle or the scission point. However, this uncertainty does not lead to any major discrepancy in the determination of the temperature. Though the excitation energies at these two different stages of the fissioning nucleus can be somewhat different, the fragment spin according to

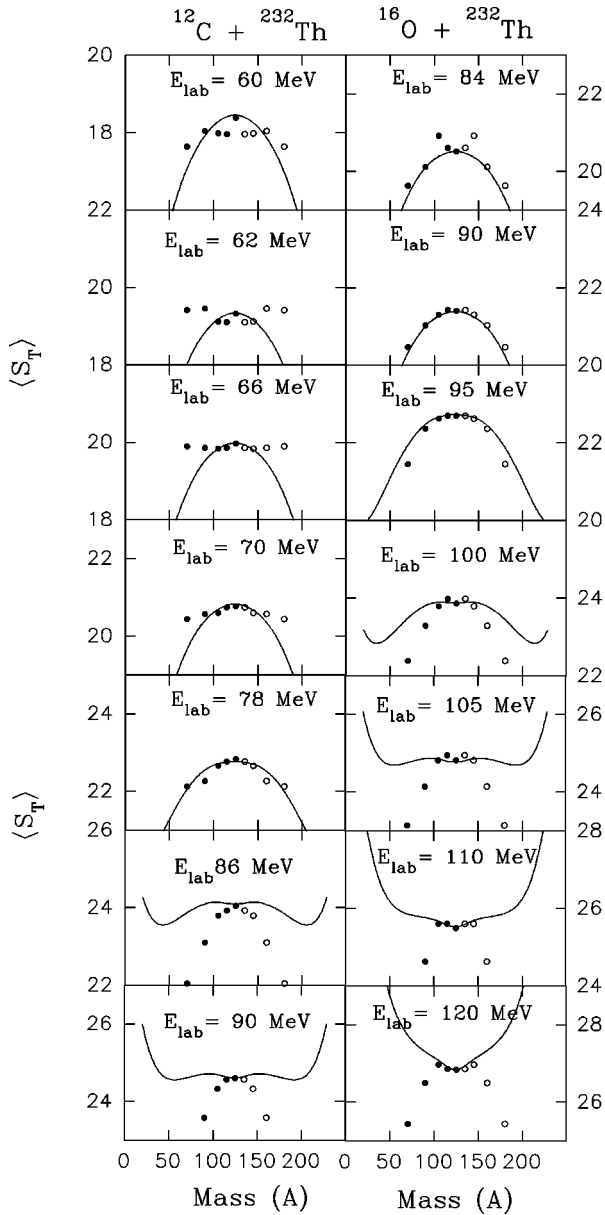


FIG. 6. Same as in Fig. 5 for  $^{12}\text{C} + ^{232}\text{Th}$  and  $^{16}\text{O} + ^{232}\text{Th}$  reactions.

the statistical model is proportional to  $T^{1/2}$  or  $(E^*)^{1/4}$ , which remains significantly unchanged over a large difference in the absolute values of excitation energies.

A typical calculation carried out for the  $^{12}\text{C} + ^{209}\text{Bi}$  reaction at  $E_{\text{lab}} = 90$  MeV using the statistical model is shown in Fig. 7, where the rigid rotation and the collective components of the angular momentum are shown as a function of fragment mass. The average total fragment spin, obtained as the quadratic sum of the two components is also shown in the figure. It is observed that the contribution of the collective-spin modes to the fragment spin is maximum for symmetric mass division. As the mass asymmetry increases, all the modes except tilting are suppressed due to the increased stiffness of the orbital motion and the decreased moment of inertia of the light fragment.

The calculations shown in Fig. 7 (as well as those shown

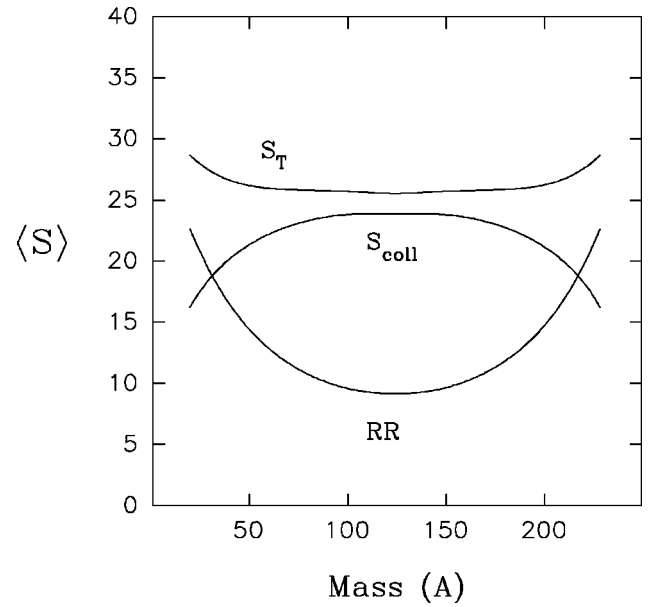


FIG. 7. Typical statistical model calculation of the mass dependence of collective spin  $S_{\text{coll}}$ , rigid rotation spin  $RR$  and the total fragment spin  $S_T$  for  $E_{\text{lab}} = 90$  MeV,  $^{12}\text{C} + ^{209}\text{Bi}$  reaction.

in Figs. 5 and 6) correspond to the spherical shapes of the fission fragments. However, it was found that [17], by using deformed shapes as would be required to reproduce the observed total kinetic energies given by the Viola systematics [26], the overall features still remain the same. The absolute spin values for the two shapes show marginal difference. For the purpose of the following discussions, we restrict ourselves to the results obtained using spherical shapes of the fragments without involving any deformation for calculation of the moment of inertia of the fragments.

#### IV. DISCUSSION

As can be seen from Figs. 5 and 6, the statistical model calculations correctly predict the mass dependence of the total fragment spin for the  $^{12}\text{C}$ ,  $^{16}\text{O} + ^{209}\text{Bi}$  reactions over a broad energy range except at the highest energies, where the experimental data show weak mass dependence but the statistical model predicts a  $u$ -type behavior. In the case of the  $^{12}\text{C}$ ,  $^{16}\text{O} + ^{232}\text{Th}$  reactions, the calculations are in disagreement with the experimental behavior for most of the energies. The discrepancy between the measurements and the calculations increase with increasing projectile bombarding energy. The experimentally determined fragment spin as a function of fragment mass in the  $^{232}\text{Th}$  systems exhibits an  $n$ -shaped behavior, in contrast to the  $u$ -shaped dependence predicted by the statistical model calculations.

As discussed earlier by Back *et al.* [17], the observed  $n$ -shaped feature in the mass dependence of fragment spin can be explained by taking into account the finite relaxation time of the collective angular momentum bearing modes. One assumes that the fissioning system equilibrates two macroscopic variables, i.e., spin  $S$  and mass  $M$ , through a diffusion process. Subject to the constraint of total angular momentum, the diffusion will tend towards a statistical

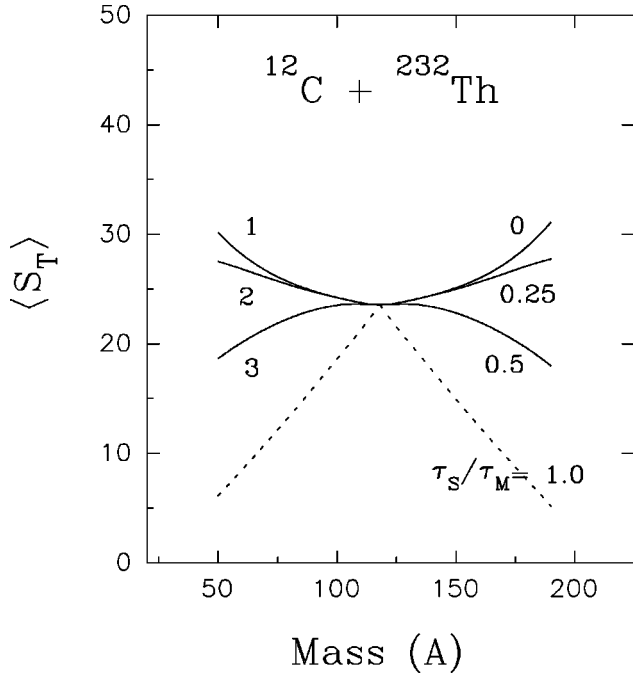


FIG. 8. Incomplete relaxation of collective-spin modes. The different curves labeled, are discussed in the text.

equilibrium with  $S$  going from  $S=0$  towards the value  $S = S_{\text{eq}}$ , and  $M$  from its initial value  $M = M_0$  towards the value  $M = M_{\text{eq}}$ , with relaxation times  $\tau_S$  and  $\tau_M$ , respectively:

$$S = S_{\text{eq}} \left[ 1 - \exp\left(-\frac{t}{\tau_S}\right) \right], \quad (5)$$

$$M = M_{\text{eq}} + (M_0 - M_{\text{eq}}) \exp\left[-\frac{t}{\tau_M}\right]. \quad (6)$$

It is known from the damped heavy-ion collisions that the mass drift towards symmetry can be well understood as an exponential relaxation process using the above relations. It has been found [27] that a universal relaxation time of  $\tau_M = 5 \times 10^{-21}$  s gives a good description of the data, independent of beam energy as well as the target mass.

Equations (5) and (6) can be recast to give fragment spin  $S$  as a power-law function of  $M$

$$S = S_{\text{eq}} \left[ 1 - \left( \frac{|M_{\text{eq}} - M|}{|M_{\text{eq}} - M_0|} \right)^{\tau_M/\tau_S} \right]. \quad (7)$$

As pointed out by Back *et al.* [17], the n-shaped curve observed experimentally could be explained by considering a spin-relaxation time of the order of  $\tau_S \sim 1/3\tau_M$ .

The above calculations can, in principle, be carried out by ascribing separate relaxation times for each of the collective-

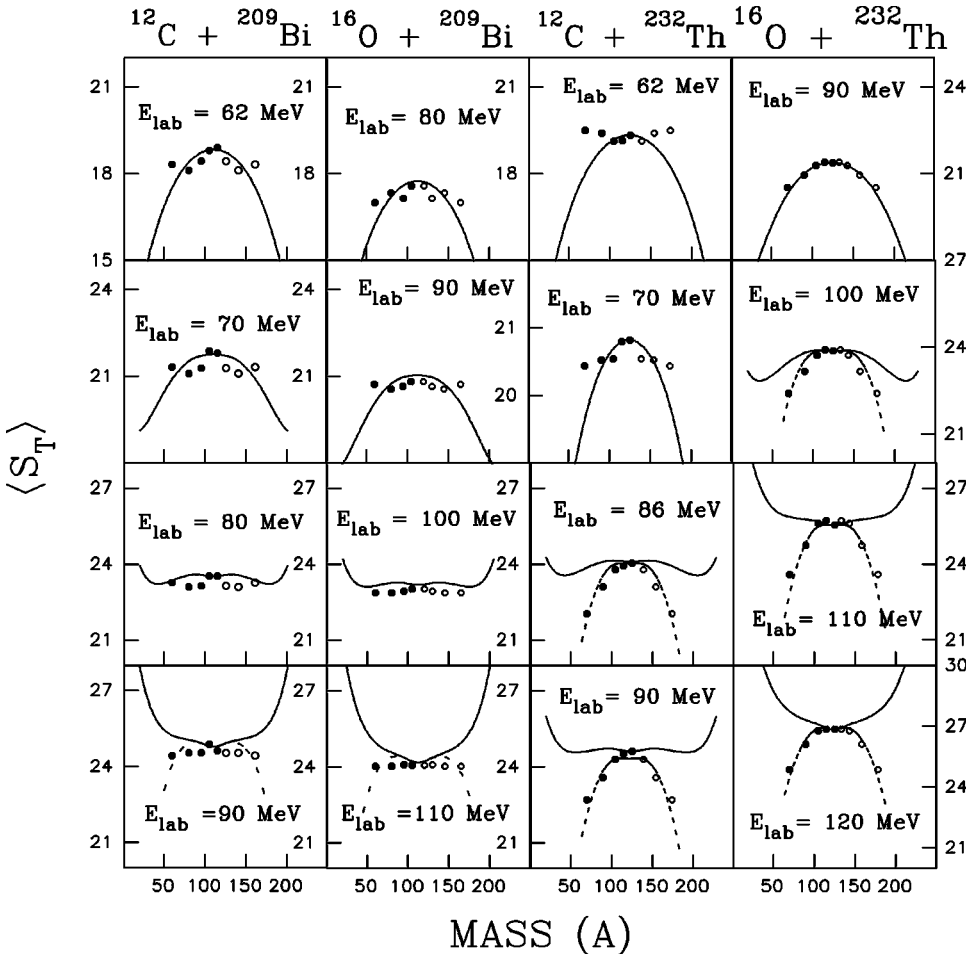


FIG. 9. Average total fragment spin as a function of mass for all the reactions studied. The dashed lines correspond to calculations using relaxation times as described in the text.

spin modes. The calculations shown by solid lines in Figs. 5 and 6 correspond to a set of typical relaxation times given by the one-body window dissipation obtained from the work of Dossing and Randrup [28]. With typical mass relaxation time of  $\tau_M \approx 5 \times 10^{-21}$  s, the typical relaxation times for various collective-spin modes predicted are: wriggling  $\tau_S/\tau_M \approx 0.05$ , bending and twisting  $\tau_S/\tau_M \approx 0.2$ , tilting  $\tau_S/\tau_M \approx 2.0$ . Since the total spin is derived from the quadratic sum of the spins due to various modes, the shape of the mass dependence of fragment spin is mainly governed by the collective mode having the fastest relaxation time. Thus the spin distribution away from symmetry is mainly dominated by the wriggling mode. It is seen that, to explain the observed n-shaped feature in mass dependence of fragment spin, one needs the spin-relaxation times to be about ten times larger than that calculated from the window dissipation model, as shown by the curve labeled 3 in Fig. 8, where  $\tau_S/\tau_M$  values labeling the curves correspond to those used for the wriggling mode.

Statistical model calculations were carried out for the  $^{12}\text{C}$ ,  $^{16}\text{O}+^{232}\text{Th}$  reactions with increased spin relaxation times over the energy range studied in the present work and the results are shown in Fig. 9. In case of  $^{209}\text{Bi}$  systems, the increased spin-relaxation time was used only for the highest energies, where deviations were observed between experimental data and the statistical model calculations. The calculations were done with spin-relaxation times of about 6–8 times larger than that predicted by the one-body dissipation model for wriggling, bending, and twisting. It is seen that with longer spin-relaxation times, one is able to explain the experimental results to a better extent.

The collective-spin modes for  $^{12}\text{C}$  and  $^{16}\text{O}+^{232}\text{Th}$  reactions thus appear to be excited with characteristic times that are longer than the reaction time, and substantially longer than that expected on the basis of the window dissipation model. The mass relaxation process at extreme mass asymmetries for these heavy fissioning systems seems to terminate before full statistical equilibrium of some of the

collective-spin modes is reached. This result may imply the presence of pre-equilibrium fission modes at large mass asymmetries in these reactions.

## V. SUMMARY AND CONCLUSION

In summary, we have carried out systematic measurements of the fission fragment spins as a function of fragment mass in  $^{12}\text{C}$ ,  $^{16}\text{O}+^{209}\text{Bi}$  and  $^{12}\text{C}$ ,  $^{16}\text{O}+^{232}\text{Th}$  reactions. The data were obtained over a large range of bombarding energies near and above the Coulomb barrier for all the systems. The experimentally observed mass dependence of fission fragment spins for  $^{12}\text{C}$ ,  $^{16}\text{O}+^{232}\text{Th}$  reactions is in marked contrast to that for  $^{12}\text{C}$ ,  $^{16}\text{O}+^{209}\text{Bi}$  reactions. The present results were analyzed within the statistical model for complete equilibration of the collective-spin modes. It is found that while the statistical assumption of complete equilibration of the collective-spin modes is valid for  $^{12}\text{C}$ ,  $^{16}\text{O}+^{209}\text{Bi}$  reactions to a large extent, the same is not true for the  $^{12}\text{C}$ ,  $^{16}\text{O}+^{232}\text{Th}$  reactions. The n-shaped mass dependence of fragment spin in  $^{12}\text{C}$ ,  $^{16}\text{O}+^{232}\text{Th}$  reactions implies incomplete equilibration of the collective-spin modes for extreme mass asymmetries. The experimental data at higher bombarding energies can only be explained by taking into account the finite relaxation time for the equilibration of the collective-spin modes. It is observed that one needs spin-relaxation times about 6–8 times larger than that calculated from the one-body window dissipation model. These results imply that for the heavy fissioning systems at high excitation energies, the collective-spin modes are damped and the fragments with large mass asymmetries are formed without full equilibration of the fragment spins.

## ACKNOWLEDGMENTS

The authors are grateful to the staff of the LNL tandem laboratory for providing the good quality beams required for the experiment.

- 
- [1] L. G. Moretto and R. P. Schmitt, *Phys. Rev. C* **21**, 204 (1980).
  - [2] R. P. Schmitt, G. Mouchaty, and D. R. Haenni, *Nucl. Phys.* **A427**, 614 (1984).
  - [3] R. Bock *et al.*, *Nucl. Phys.* **A388**, 334 (1982).
  - [4] F. Dilmanian, L. Grozins, J. W. Ball, M. Beckerman, R. Boisseau, S. Gazes, R. Ledoux, and A. Sperduto, *Phys. Lett.* **127B**, 172 (1983).
  - [5] R. P. Schmitt, G. Mouchaty, D. R. Haenni, and M. Tirion, *Z. Phys. A* **321**, 411 (1985).
  - [6] V. S. Ramamurthy *et al.*, *Phys. Rev. Lett.* **65**, 25 (1990).
  - [7] N. Majumdar, P. Bhattacharya, D. C. Biswas, R. K. Choudhury, D. M. Nadkarni, and A. Saxena, *Phys. Rev. C* **51**, 3109 (1995).
  - [8] N. Majumdar, P. Bhattacharya, D. C. Biswas, R. K. Choudhury, D. M. Nadkarni, and A. Saxena, *Phys. Rev. C* **53**, R544 (1996).
  - [9] N. Majumdar, P. Bhattacharya, D. C. Biswas, R. K. Choudhury, D. M. Nadkarni, and A. Saxena, *Phys. Rev. Lett.* **77**, 5027 (1996).
  - [10] A. Karnik *et al.*, *Z. Phys. A* **351**, 195 (1995).
  - [11] R. Vandenbosch *et al.*, *Phys. Rev. C* **54**, R977 (1996).
  - [12] D. J. Hinde, M. Dasgupta, J. R. Leigh, J. P. Lestone, J. C. Mein, C. R. Morton, J. O. Newton, and H. Timmers, *Phys. Rev. Lett.* **74**, 1295 (1995).
  - [13] Z. Liu *et al.*, *Phys. Lett. B* **353**, 173 (1995).
  - [14] J. C. Mein, D. J. Hinde, M. Dasgupta, J. R. Leigh, J. O. Newton, and H. Timmers, *Phys. Rev. C* **55**, R995 (1997).
  - [15] D. J. Hinde, M. Dasgupta, J. R. Leigh, J. C. Mein, C. R. Morton, J. O. Newton, and H. Timmers, *Phys. Rev. C* **53**, 1290 (1996).
  - [16] Y. El. Masri *et al.*, *Nucl. Phys.* **A517**, 340 (1990).
  - [17] B. B. Back *et al.*, *Phys. Rev. C* **41**, 1495 (1990).

- [18] D. Bazzacco, in *Proceedings of the International Conference on High Angular Momentum*, Ottawa, 1992 (AECL Research, Chalk River, Ontario, Canada, 1992), Vol. 2, p. 376.
- [19] J. Fernandez-Neillo, C. H. Dasso, and S. Landowne, *Comput. Phys. Commun.* **54**, 409 (1989).
- [20] A. Ya. Rusanov, M. G. Itkis, and V. N. Okolovich, *Yad. Fiz.* **60**, 773 (1997) [*Phys. At. Nucl.* **60**, 683 (1997)].
- [21] W. J. Ockels, *Z. Phys. A* **286**, 181 (1978).
- [22] D. V. Shetty, R. K. Choudhury, B. K. Nayak, D. M. Nadkarni, and S. S. Kapoor, *Phys. Rev. C* **58**, R616 (1998).
- [23] R. P. Schmitt, L. Cooke, H. Dejbakhsh, D. R. Haenni, B. K. Srivastava, and H. Utsunomiya, *Nucl. Phys.* **A592**, 130 (1995).
- [24] D. V. Shetty, R. K. Choudhury, B. K. Nayak, D. M. Nadkarni, and S. S. Kapoor, *Phys. Rev. C* **56**, 868 (1997).
- [25] R. P. Schmitt and A. J. Pacheco, *Nucl. Phys.* **A379**, 313 (1982).
- [26] V. E. Viola, Jr., K. Kwiatowski, and M. Walker, *Phys. Rev. C* **31**, 1550 (1985).
- [27] W. Q. Shen *et al.*, *Phys. Rev. C* **36**, 115 (1987).
- [28] T. Dossing and J. Randrup, *Nucl. Phys.* **A433**, 215 (1985); **A433**, 280 (1985).